Zoological Journal of the Linnean Society, 2005, **144**, 309–316. With 2 figures

Aspects of comparative cranial mechanics in the theropod dinosaurs *Coelophysis, Allosaurus* and *Tyrannosaurus*

E. J. RAYFIELD*

Department of Earth Sciences, University of Cambridge, Downing Street, Cambridge, CB2 3EQ, UK

Received June 2004; accepted for publication March 2005

The engineering analysis technique finite element analysis (FEA) is used here to investigate cranial stress and strain during biting and feeding in three phylogenetically disparate theropod taxa: *Coelophysis bauri*, *Allosaurus fragilis* and *Tyrannosaurus rex*. Stress patterns are generally similar in all taxa with the ventral region of the skull tensed whilst the dorsal aspect is compressed, although the skull is not purely behaving as a cantilever beam as there is no discernible neutral region of bending. Despite similarities, stress patterns are not wholly comparable: there are key differences in how certain regions of the skull contain stress, and it is possible to link such differences to cranial morphology. In particular, nasal morphology can be explained by the stress patterns revealed here. *Tyrannosaurus* models shear and compress mainly in the nasal region, in keeping with the indistinguishably fused and expanded morphology of the nasal bones. Conversely *Allosaurus* and *Coelophysis* models experience peak shear and compression in the fronto-parietal region (which is tightly interdigitated and thickened in the case of *Allosaurus*) yet in contrast the nasal region is lightly stressed, corresponding to relatively gracile nasals and a frequently patent internasal suture evident in *Allosaurus*. Such differences represent alternate mechanical specializations between taxa that may be controlled by functional, phylogenetic or mechanical constraints. Creation of finite element models placed in a phylogenetic context permits the investigation of the role of such mechanical character complexes in the cranium of nonavian theropods and the lineage leading towards modern birds. *Zoological Journal of the Linnean Society*, 2005, **144**, 309–316.

ADDITIONAL KEYWORDS: bite force – Dinosauria – feeding – finite element analysis – skull – strain – stress – Theropoda.

INTRODUCTION

Functional behaviours such as feeding, respiration and fighting impart loads upon the vertebrate cranium that stress and strain the bones and soft tissues of the head. Cranial bones possess a number of structural features apparently associated with stress and strain resistance, transmission and dissipation, such as sutures, trabeculation, material property distribution and bone thickenings or reduction (Oxnard, 1971; Buckland-Wright, 1978; Thomason & Russell, 1986; Jaslow, 1990; Jaslow & Biewener, 1995; Herring, 2000; Rayfield *et al*., 2001; Rafferty, Herring & Marshall, 2003). Such features modify the stress and strain environment of the skull and as a result may serve as indicators of loading patterns and functional behaviour (Rafferty & Herring, 1999; Rayfield *et al*., 2001; Jenkins, Thomason & Norman, 2002).

This paper investigates the mechanical behaviour of the crania of three taxonomically disparate theropod dinosaurs in response to feeding loads, in order to begin deciphering the evolution of structural mechanisms in place to contain cranial stress and strain in theropods and their avian descendants. Non-avian theropod dinosaurs are interesting test cases: their endocranium in all except maybe the most derived forms is proportionally much smaller relative to overall skull size than it is in mammals or birds (Larsson, Sereno & Wilson, 2000; Domínguez Alonso *et al*., 2004) As such, functional constraints imposed by enclosure of the brain and sense organs (Demes, 1982; Thomason, 1991) may be lessened in theropods, resulting in

*Current address: Department of Palaeontology, The Natural History Museum, Cromwell Road, London, SW7 5BD, UK. E-mail: e.rayfield@nhm.ac.uk

fewer constraints when accommodating feeding forces (although some cranial features have been linked to pneumatization by Witmer, 1997). For example, the lateral sidewalls of the skull are, in many theropod taxa, reduced to a series of interconnected struts enclosing expansive fenestrae and in the case of large theropods such as *Tyrannosaurus rex* Osborn, 1905 and *Allosaurus fragilis* Marsh, 1877, these features appear to be linked with the resistance of extremely large biting forces (Erickson *et al*., 1996; Rayfield, 2004) or cranial loading (Rayfield *et al*., 2001).

Finite element analysis (FEA) is an engineering computer-based technique capable of calculating stress and strain within structures in response to applied loads. Here it is used in the manner employed by Rayfield (2004) and Rayfield *et al*. (2001) to calculate and compare stress and strain in the cranium of taxonomically disparate and to a certain extent structurally distinct theropods: *Coelophysis bauri*, *Allosaurus fragilis* and *Tyrannosaurus rex* (Fig. 1A, B, C). The largest *Coelophysis* skulls are under 300 mm rostrum to occipital length. They are transversely narrow with

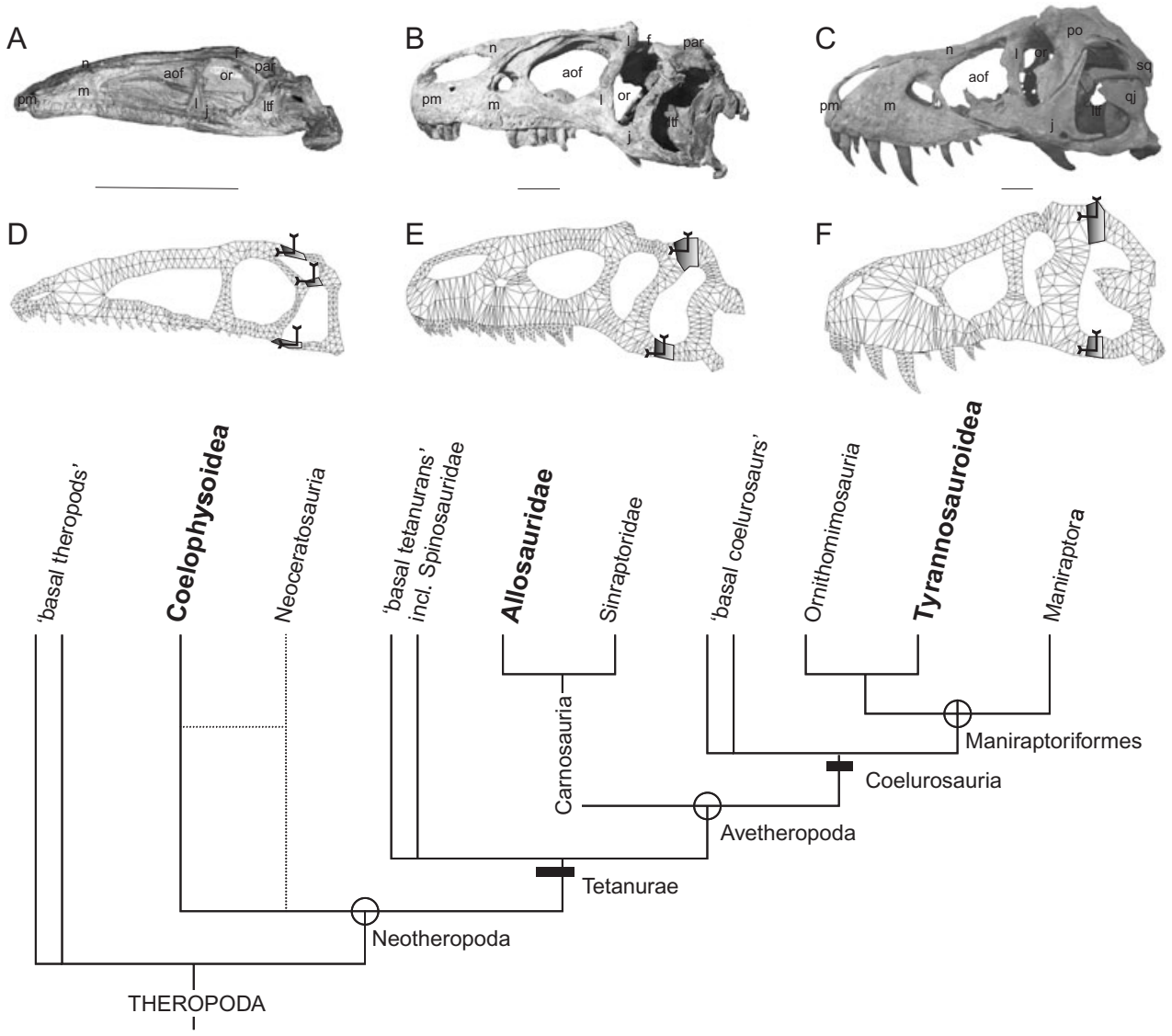

Figure 1. Finite element (FE) models created in this study with respect to taxonomic position with the Theropoda. From left to right: A, *Coelophysis bauri*, skull and D, FEA model; B, *Allosaurus fragilis*, skull and E, FEA model; C, *Tyrannosaurus rex*, skull and F, FEA model. Grey patches on mesh indicate constrained region of model (in direction indicated by arrows). Scale bar = 10 cm. Phylogeny adapted from Holtz (2000) and Rauhut (2003); open circles indicate node-based taxa; black lines indicate stem-based taxa. *Abbreviations*: aof, antorbital fenestra; f, frontal; j, jugal; l, lacrimal; ltf, lower temporal fenestra; m, maxilla; n, nasal; or, orbit; par, parietal; po, postorbital; pm, premaxilla; qj, quadratojugal; sq, squamosal.

large antorbital fenestrae and orbits and the jaws bear small, uniform recurved teeth. *Allosaurus* possesses a large cranium (700–800 mm adult length), and fenestrae and orbits that are reduced in proportion relative to *Coelophysis*. Teeth contained with the robust maxillae become progressively medio-laterally compressed towards the rear of the toothrow (Madsen, 1976; Rayfield *et al*., 2001). *Tyrannosaurus* possesses extremely robust, transversely expanded crania with stout interfenestral bars that encroach into the orbit and lower temporal fenestrae. Positional variability in tooth form is observed, with U-shaped premaxillary teeth and maxillary teeth becoming stout, almost conical in morphology (Farlow *et al*., 1991; Molnar, 1998; Hurum & Sabath, 2003).

The aim of this analysis was to compare the mechanical performance of crania during biting, and identify similarities and differences in stress and strain distribution and orientation between taxa. It was hypothesized that differences in stress/strain patterns may be linked to morphological features that in turn may represent alternate mechanical and possibly functional specializations between taxa. Alternatively, stress/strain patterns may conform in all three models, reflecting similar mechanical parameters (that may be phylogenetically or otherwise constrained) or the fact that stress flows within the cranium are opportunistic (*sensu* Preuschoft & Witzel, 2002), with stress disseminating throughout all available bony tissue. Furthermore, if the skull behaves as a beam during biting (Molnar, 1998), the dorsal skull will be compressed as the ventral skull is tensed and the interfenestral bars that lie about the neutral axis of bending should experience little or no stress.

MATERIAL AND METHODS

In this study, two-dimensional FE models were created to represent the near-planar morphology of the lateral walls of the theropod cranium. 2D FE models are commonly used as a first approximation in biomechanical modelling (Carter, Mikic & Padian, 1998) as producing simple FE models reduces assembly time and offers the possibility to devise functional hypotheses that may be tested later in more geometrically or materially sophisticated models.

The generation of 2D *Tyrannosaurus* FE models was discussed in Rayfield (2004). Here the *Allosaurus* and *Coelophysis* 2D models were produced in the same manner. Lateral aspect photographs (taken by the author, Fig. 1) of *Tyrannosaurus rex* BHI 3033 (Black Hills Institute, Hill City, South Dakota); *Allosaurus fragilis* DNM 2560 (Dinosaur National Monument, Vernal, Utah) and *Coelophysis bauri* CM 31374 (Carnegie Museum of Natural History) were digitized in Scion Image (http://www.scioncorp.com). Outline x,y co-ordinates were imported into the Geostar geometry creator component of CosmosM Finite Element Analysis (FEA) package (v. 2.8, SRAC, Ca. USA and Cenit Ltd, UK). A series of 50 mm thick surfaces were created then 'meshed' to produce an interconnected grid of triangular 3-noded finite elements representing the lateral aspect of the crania (Fig. 1D, E, F). The *Tyrannosaurus* model comprised 820 elements; the *Allosaurus* model comprised 935 and the *Coelophysis* model comprised 671. Each element was attributed the mechanical properties of bovine Haversian bone after Rayfield *et al*. (2001). The models were constrained from movement about surfaces dorsal and ventral to the lower temporal fenestra (Fig. 1D, E, F) so stress patterns posterior to this region should be disregarded. Error encountered when modelling the posterior skull region in two dimensions is therefore reduced and muscular and condylar forces are not applied.

Asymmetrical patterns of cranial stress generated during unilateral biting (Rayfield, 2001) cannot be visualized in 2D models, therefore the models presented here assume that biting is bilateral. It is possible to estimate absolute forces experienced at the teeth during adductor-generated biting in theropods (as in Rayfield *et al*., 2001 for *Allosaurus*), and as such these forces were applied to the teeth of the 2D *Allosaurus* model (giving a total bite force of 27 238 N). The *Tyrannosaurus* models assessed here are those figured in Rayfield (2004) in which a total of 78 060 N bite force was applied across all teeth, based on an extrapolation of estimated single tooth bite forces calculated by Erickson *et al*. (1996). *Coelophysis* bite forces are unestimated, therefore 535 N, close to the maximum biting force of an opossum (Thomason, Russell & Morgeli, 1990) was divided unequally between all 22 teeth of *Coelophysis bauri* CM 31374. This analysis does not purport to visualize absolute cranial stress and strain in dinosaur crania during biting, instead the application of reasonably realistic bite forces is an attempt to generate useful comparative models in which relative similarities and differences in mechanical behaviour may be observed. However as a comparison, three further load cases were defined, in which each skull was loaded with 10 000 N of bite force (divided between all teeth participating in the bite). These latter models enable a blanket comparison of relative cranial stress across taxa, similar to the approach employed by Henderson (2002) in examining skull strength in theropods. All bite forces were vertically, dorsally directed.

Stress and strain within the skull in response to the applied bite loads and constraints was analysed for all three models using the STAR FEA solver of CosmosM. Results were visualized and assessed using post-processing package tools in Geostar.

RESULTS

Colour stress distribution and vector orientation plots illustrate the pattern of stress and strain in the skull under biting loads. Principal stress vector orientation is indicated by diverging arrows for tension and converging arrows for compression. By convention tensile stresses and strains are ascribed positive values, whilst compressive stresses and strains are assigned negative values. Care should be taken when reading stress plots as the scale bar varies such that the same colour can represent tension or compression in different plots. It is the case, however, that areas of zero stress or strain are always the same shade as the region posterior to the constraining surfaces, which due to the location of constraint is not loaded. Principal stresses (P1 tensile; P3 compressive), shear stress in the sagittal (here XY) 2D plane, normal X, normal Y and sagittal XY shear strain were recorded. Principal stresses record peak compressive and tensile stresses when shear stress equals zero.

Tensile and compressive stress

Intraspecific stress distribution is similar during estimated biting or blanket loading regimes, although absolute stress magnitudes vary. Interspecifically, general patterns of tensile and compressive stress are similar in all models. A dorsally directed bite load leads to compressive load vectors arching posterodorsally through the maxilla into the nasals and the dorsal aspect of the lacrimals. Dorsally stress orientation becomes longitudinally orientated, and stresses continue into the frontal and parietal of the skull roof. (Fig. 2A, B, C). The premaxilla and nasals dorsal to the external naris are compressed slightly in *Allosaurus* (Fig. 2B), but not obviously stressed in *Tyrannosaurus* and *Coelophysis* (Fig. 2A, C). The diastema between premaxilla and maxilla in *Coelophysis* appears to have little effect on the distribution of bite loads (Fig. 2A, D, G).

A key difference between the *Tyrannosaurus* cranium and those of *Allosaurus* and *Coelophysis* is that whilst peak compressive stresses are found dorsal to the antorbital fenestra in the former (Rayfield, 2004), the fronto-parietal region is the location of peak compression in *Allosaurus* and *Coelophysis* (Fig. 2C, cf. Fig. 2A, B). Large compressive stresses are also found in the postorbital region of *Tyrannosaurus* (Fig. 2C; Rayfield, 2004: figs 3, 4) whilst *Allosaurus* and *Coelophysis* postorbitals are not highly compressed (Fig. 2A, B).

In all models peak tensile stresses are found ventral to the orbit and antorbital fenestra, with the main body of the jugal experiencing the majority of tensile stress, with the posterior region of the maxillae also being tensed (Fig. 2D, E, F). Tensile vectors follow the ventral rim of the jugal then orientate anterodorsally to track the ventral rim of the antorbital fenestra and maxillary fenestra (where present). This leaves the robust main body of the maxilla dorsal to the tooth row relatively untensed.

The lacrimal of all models experiences complex stress patterns of anterodorsal-posteroventrally orientated tension criss-crossing with posterodorsal-anteroventrally orientated compressive vectors (Fig. 2A–C and D–F). The net result of compressive and tensile vector orientation about the lacrimal and the antorbital fenestra is that the anterior, dorsal and to some extent posterior margins of the fenestra are compressed, whilst the ventral margin is tensed. The stress environment encircling the orbit is more ambiguous: compressive vectors in the postorbital bar of *Allosaurus* and *Tyrannosaurus* ensure that the orbital margins are mainly compressed in these taxa (Fig. 2B, C) but the postorbital of *Coelophysis* is unstressed (Fig. 2A); a phenomenon either associated with the large orbit or an erroneous result due to the proximity of the constraining surfaces.

Shear stress

Shear stresses reveal clearer distinctions between the stress environment of each model. *Allosaurus* and *Coelophysis* tend to shear along the ventral edge of the skull, mainly in the region of the jugal (Fig. 2G, H). *Allosaurus* also experiences large shear about the anterior, ventral and posterior margins of the antorbital fenestra, with some shear also experienced in the fronto-parietal region (Fig. 2H). Whilst the *Tyrannosaurus* model also shears in the jugal region, and about the anterior antorbital fenestra and maxillary fenestra, peak shear stresses are instead found dorsal to the antorbital fenestra and orbit, in the nasals, lacrimal, frontal and dorsal postorbital (Fig. 2I; Rayfield, 2004: figs 3, 4). In stark contrast, the nasals and lacrimal of *Coelophysis* and *Allosaurus* are regions of low shear stress (Fig. 2G, H). Shear strain plots display the same results.

DISCUSSION

Finite element modelling reveals that general similarities in cranial morphology: the possession of antorbital fenestrae, large orbits and lower temporal fenestrae and an elongated snout, appear to lead to similarities in stress distribution between the crania of *Allosaurus*, *Tyrannosaurus* and *Coelophysis*. There are, however, key differences in how stress is accommodated within the skull, meaning that subtle differences in cranial morphology can generate mechanical responses that may be related to feeding or some other

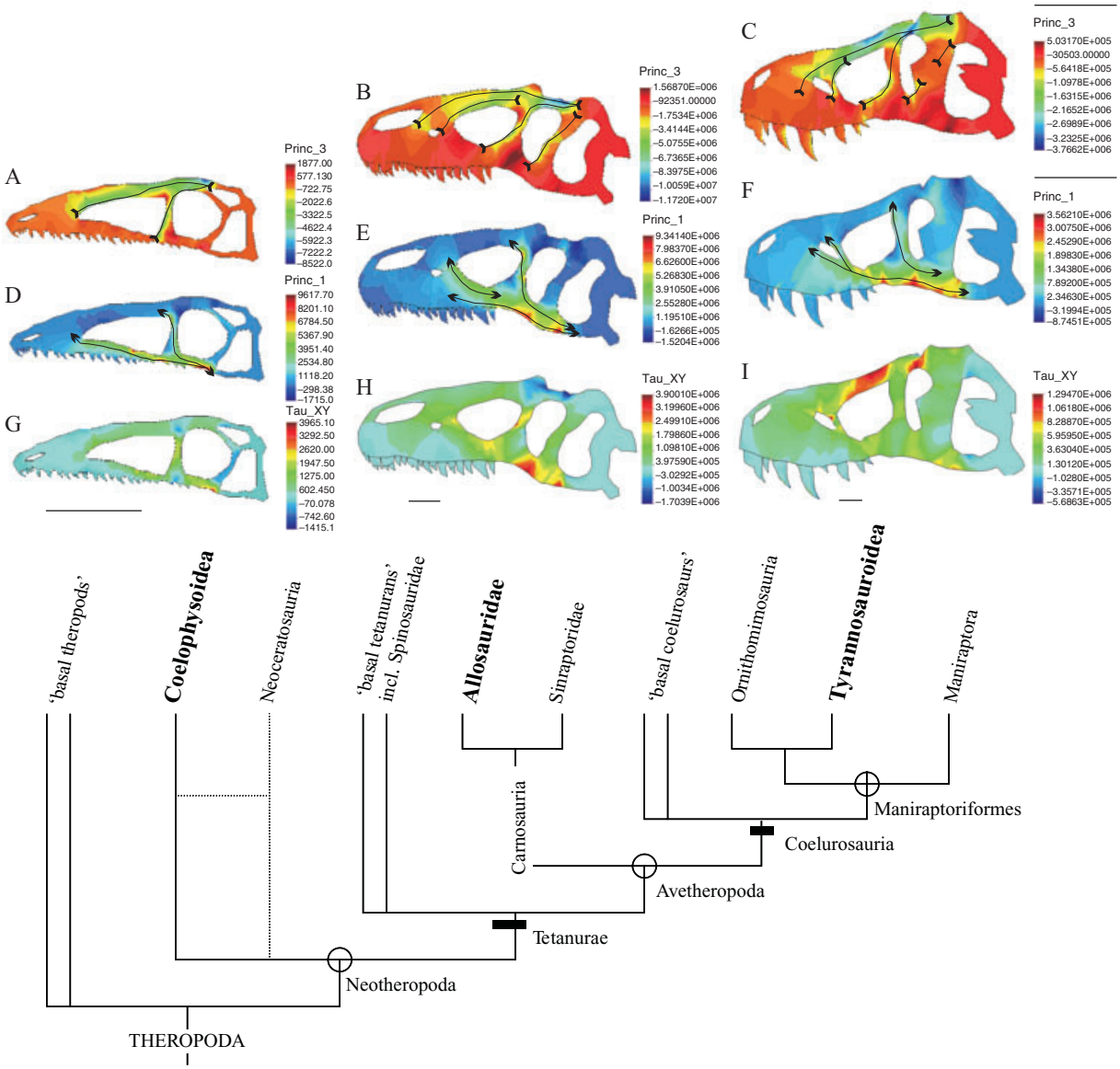

Figure 2. Stress distribution within the crania of *Coelophysis* (A, D, G), *Allosaurus* (B, E, H) and *Tyrannosaurus* (C, F, I) during bite loading. See scale for stress type and magnitude (tension is positive; compression negative); units are Pascals (1 Pa = 1 N/m^2). A–C, principal stress 3, mainly compression; D–F: principal stress 1, mainly tensile; G–I, In-plane shear stress (Tau XY). Divergent arrows indicate orientation of tensile stress, convergent arrows indicate orientation of compressive stress, phylogeny as for Fig. 1. 10 000 N bite load applied to all models.

functional or indeed nonfunctional difference between taxa. Stress flows do not extend into every available region of bone, strain gradients exist, therefore stresses are not wholly opportunistic in their distribution under this modelled loading regime (although many other loading regimes must be tested before discarding the opportunistic hypothesis). Although the skull is tensed ventrally and compressed dorsally, the interfenestral bars lying in the supposed neutral region are tensed compressed and sheared too, so the skull does not simply bend as a cantilever beam during bite loading.

Patterns of shear and compressive stress tend to be similar in *Allosaurus* and *Coelophysis*, but distinct from the patterns observed in the *Tyrannosaurus* skull. It has been shown previously that *Tyrannosaurus* nasal robusticity and fusion may be related to compressive and shear stress accumulating in this region of the cranium during a bite (Rayfield, 2004; recently suggested by Snively & Henderson, 2004). In

comparison, peak compression and shear localize to the fronto-pareital region in *Allosaurus* and *Coelophysis*, whilst the nasals and lacrimals dorsal to the antorbital fenestra experience lower magnitude stresses. In *Allosaurus* the frontals and parietals are thickened elements, tightly sutured at their midline and to each other. In sharp contrast to the rugose, fused nasals observed in tyrannosaurids, the nasals (and lacrimals) of *Allosaurus* are laterally rugose, pneumatized and elevated, yet medially comprise smooth, flattened sheets of bone that generally remain patent at the internasal suture. The prefrontal of *Allosaurus*, although short in ventral aspect and wedge-like, has an anterior expansion that forms an integral component of the dorsal skull roof, articulating with the lacrimal, nasal and frontal. Again, in contrast, the prefrontals of *Tyrannosaurus* are extremely reduced in size (Hurum & Sabath, 2003), possibly as an adaptation to increase stability and reduce intracranial weakness in the heavily stressed nasal-lacrimal-frontal region. It appears that differential localization of stress predicted by the FE-models is linked to differences in nasal and skull roof morphology between *Tyrannosaurus* and *Allosaurus*.

Further correlations between stress patterns and cranial morphology are observed in the lacrimals. In *Allosaurus* and *Tyrannosaurus*, a thin but medially prominent ridge runs confluent to the posterodorsal-anteroventral axis of compressive stress observed in the 2D models (Madsen, 1976; Rayfield, 2001, 2004; Hurum & Sabath, 2003) and possibly acts to resist elevated stresses. With the exception of this ridge, the lacrimals are medially excavated, yet a lateral shelf and anteriorly extending lip of bone runs roughly confluent to the axis of tensile stress and may be responsible for tensile strain resistance. Laterally, the ventral lacrimal of *Coelophysis* is triangular in shape, thin centrally but with prominent anterior and posterior ridges running along the axes of tensile and compressive stress generated by the model.

The jugal experiences high magnitude tensile stress in all taxa and large shearing stress in *Allosaurus* and *Coelophysis*. Interestingly, *Tyrannosaurus* jugals are exceptionally bulbous and robust, yet shear stresses are low in this region compared to the other two taxa. This perhaps supports the idea that at least some of the robustness of the *Tyrannosaurus* jugal may be attributed more to transverse cranial expansion in this region and the incorporation of pneumaticity (Molnar, 1991) and possibly increased adductor musculature, rather than to stress resistance.

Tensile stress along the ventral edge of the antorbital fenestra is counteracted by compressive stresses encircling the remainder of the fenestrae. This action may serve to strengthen the fenestra and enhance their role as stress-resisting features within the skull (observed as 'stress loops' in the 3D *Allosaurus* model, Rayfield *et al*., 2001). Thickened tracts of the bone demarcating the edges of the fenestra and the antorbital fossa of *Allosaurus* and *Coelophysis* may be structural constructs to compensate for structural weakness initiated by the introduction or expansion of an opening to a plate of bone. Stresses are channelled anteriorly and posteriorly around the maxillary fenestra, where present.

The general pattern of stress distribution found in these 2D models: compression arcing from the biting teeth to the skull roof while the ventral skull is tensed, is corroborated by the appearance of similar patterns in 3D FE models of *Allosaurus* crania (Rayfield *et al*., 2001). Further 3D models are needed to account for differences in mediolateral thickness between bones and possible bending moments in the transverse plane, which are assumed here in these models to be negligible due to the dorsoventrally expanded, mediolaterally narrow aspect of the theropod skull, yet this must be tested. Although further comparison of FE models against extant strain data is needed to verify model output further, FEA stress trajectories presented here trace patterns of structural continua observed in extant crania (Buckland-Wright, 1978; Roberts, 1979) and in some cases are similar in orientation to *in vivo* strain data (Thomason *et al*., 2001: figs 5, 7), although phylogenetic and functional differences in strain orientation exist (Ravosa, Johnson & Hylander, 2000; Herring *et al*., 2001) and sutures disrupt strain orientation further (e.g. Rafferty *et al.*, 2003).

CONCLUSION

An investigation into the mechanical function of three taxonomically disparate theropod dinosaurs has revealed that, in general, all three animals contain and distribute biting stresses in the same basic manner. The skull is generally bent during biting so that it is ventrally tensed and dorsally compressed (which may be expected given the nature of the vertical bite force and constraining points anchoring the rear of the skull) yet the interfenestral bars do experience stress, so the cantilever beam analogy is not wholly appropriate. Despite stress distribution similarities, there are specific differences in how certain regions of the skull contain stress. This indicates that stress flows are not opportunistically expanding into all available bony tissue. Morphology (even in two dimensions) is dictating stress distribution to some extent such that differences in stress distribution may be linked to differences in cranial morphology between taxa. Differences in nasal morphology between *Allosaurus* and *Tyrannosaurus* may be explained by variation in the location of peak compression and shear. The structure of the lacrimal in all taxa may serve to counteract high

magnitude stresses, whilst prefrontal reduction in *Tyrannosaurus* may be linked to skull strengthening. Deviations in cranial stress patterns in *Tyrannosaurus* could be attributed to proportional changes shortening the preorbital skull length, and therefore shifting peak shear from the fronto-parietal in *Allosaurus* and *Coelophysis* to dorsal to the antorbital fenestra in *Tyrannosaurus*. This remains to be tested. An analysis of cranial stress distribution in other theropods with fused nasals such abelisaurids and spinosaurids may contribute to our understanding of nasal fusion vs. patency. Similarities between 2D stress patterns and those observed in living animals and realistic 3D FE models illuminate the predictive nature of simple FE models for generating hypotheses of cranial function, which may be tested using more sophisticated models in the future. Further FE modelling, in particular of sutures, muscular and condylar force application, sophisticated elastic properties (incorporating compact and cancellous bone) and incorporation of soft tissues combined with verification of model data with *in vivo* strain gauge experimentation on extant taxa will enable a fuller understanding of cranial evolution within theropod dinosaurs and the lineage leading to modern birds.

ACKNOWLEDGEMENTS

This research was undertaken with support from a junior research fellowship at Emmanuel College, Cambridge University, with additional funding from the Royal Society (equipment grant). For access to specimens I thank Elizabeth Hill (Carnegie Museum), Dan Chure (Dinosaur National Monument), Peter Larson (Black Hills Institute); for technical assistance CenitDesktop Ltd; for draft reading David Norman, and finally Tom Holtz and an anonymous reviewer for constructive review comments.

REFERENCES

Buckland-Wright JC. 1978. Bone structure and the patterns of force transmission in the cat skull (*Felis catus*). *Journal of Morphology* **155:** 35–62.

Carter DR, Mikic B, Padian K. 1998. Epigenetic mechanical factors in the evolution of long bone epiphyses. *Zoological Journal of the Linnean Society* **123:** 163–178.

Demes B. 1982. The resistance of primate skulls against mechanical stresses. *Journal of Human Evolution* **11:** 687–691.

Domínguez Alonso P, Milner AC, Ketcham RA, Cookson MJ, Rowe TB. 2004. The avian nature of the brain and inner ear of *Archaeopteryx*. *Nature* **430:** 666–669.

Erickson GM, Van Kirk SD, Su J, Levenston ME, Caler WE, Carter DR. 1996. Bite-force estimation for *Tyrannosaurus rex* from tooth-marked bones. *Nature* **382:** 706–708.

Farlow JO, Brinkman DL, Abler WL, Currie PJ. 1991. Size, shape, and serration density of theropod dinosaur lateral teeth. *Modern Geology* **16:** 161–198.

Henderson DM. 2002. The eyes have it: sizes, shapes, and orientations of theropod orbits as indicators of skull strength and bite force. *Journal of Vertebrate Paleontology* **22:** 766–778.

Herring SW. 2000. Sutures and craniosynostosis: a comparative, functional and evolutionary perspective. In: Cohen MM, MacLean RE, eds. *Craniosynostosis*, 2nd edn. Oxford: Oxford University Press, 3–10.

Herring SW, Rafferty KL, Liu ZJ, Marshall CD. 2001. Jaw muscles and the skull in mammals: the biomechanics of mastication. *Comparative Biochemistry and Physiology Part A* **131:** 207–219.

Holtz TR. 2000. A new phylogeny of the carnivorous dinosaurs. *Gaia* **15:** 5–61.

Hurum JH, Sabath K. 2003. Giant theropod dinosaurs from Asia and North America: skulls of *Tarbosaurus bataar* and *Tyrannosaurus rex* compared. *Acta Palaeontologica Polonica* **48:** 161–190.

Jaslow CR. 1990. Mechanical properties of cranial sutures. *Journal of Biomechanics* **23:** 313–321.

Jaslow CR, Biewener AA. 1995. Strain patterns in the horncores, cranial bones and sutures of goats (*Capra hircus*) during impact loading. *Journal of Zoology, London* **235:** 193–210.

Jenkins I, Thomason JJ, Norman DB. 2002. Primates and engineering principles: applications to craniodental mechanisms in ancient terrestrial predators. *Senckenbergiana Lethaea* **82:** 223–240.

Larsson HCE, Sereno PC, Wilson JA. 2000. Forebrain enlargement among nonavian dinosaurs. *Journal of Vertebrate Paleontology* **20:** 615–618.

Madsen JH Jr. 1976. *Allosaurus fragilis*: a revised osteology. *Utah Geological and Mineral Survey Bulletin* **1091:** 1–163.

Molnar RE. 1991. The cranial morphology of *Tyrannosaurus rex*. *Palaeontographica Abteilungen A* **217:** 137–176.

Molnar RE. 1998. Mechanical factors in the design of the skull of *Tyrannosaurus rex* (Osborn, 1905). *Gaia* **15:** 193–218.

Oxnard CE. 1971. Tensile forces in skeletal structures. *Journal of Morphology* **134:** 425–436.

Preuschoft H, Witzel U. 2002. Biomechanical investigations on the skulls of reptiles and mammals. *Senckenbergiana Lethaea* **82:** 207–222.

Rafferty KL, Herring SW. 1999. Craniofacial sutures: morphology, growth and *in vivo* masticatory strains. *Journal of Morphology* **242:** 167–179.

Rafferty KL, Herring SW, Marshall CD. 2003. Biomechanics of the rostrum and the role of facial sutures. *Journal of Morphology* **257:** 33–44.

Rauhut OWM. 2003. The interrelationships and evolution of basal theropod dinosaurs. *Special Papers in Palaeontology* **69:** 213.

Ravosa MJ, Johnson KR, Hylander WL. 2000. Strain in the galago facial skull. *Journal of Morphology* **245:** 51–66.

Rayfield EJ. 2001. Cranial form and function in a large theropod dinosaur: a study using Finite Element Analysis. Unpublished PhD Thesis, Cambridge University.

Rayfield EJ. 2004. Cranial mechanics and feeding in *Tyrannosaurus rex*. *Proceedings of the Royal Society of London B* **271:** 1451–1459.

Rayfield EJ, Norman DB, Horner CC, Horner JR, May Smith P, Thomason JJ, Upchurch P. 2001. Cranial design and function in a large theropod dinosaur. *Nature* **409:** 1033–1037.

Roberts D. 1979. Mechanical structure and function of the craniofacial skeleton of the domestic dog. *Acta Anatomica* **103:** 422–433.

Snively E, Henderson DM. 2004. Mechanical implications of nasal fusion in tyrannosaurid dinosaurs. *Journal of Morphology* **260:** 329 (Abstract).

Thomason JJ. 1991. Cranial strength in relation to estimated biting forces in some mammals. *Canadian Journal of Zoology-Revue Canadienne de Zoologie* **69:** 2326–2333.

Thomason JJ, Grovum LE, Deswysen AG, Bignell WW. 2001. *In vivo* surface strain and stereology of the frontal and maxillary bones of sheep: implications for the structural design of the mammalian skull. *Anatomical Record* **264:** 325–338.

Thomason JJ, Russell AP. 1986. Mechanical factors in the evolution of the mammalian secondary palate – a theoretical analysis. *Journal of Morphology* **189:** 199–213.

Thomason JJ, Russell AP, Morgeli M. 1990. Forces of biting, body size, and masticatory muscle tension in the opossum *Didelphis virginiana*. *Canadian Journal of Zoology* **68:** 318–324.

Witmer LM. 1997. The evolution of the antorbital cavity of archosaurs: a study in soft-tissue reconstruction in the fossil record with an analysis of the function of pneumaticity. *Journal of Vertebrate Paleontology 17 (Suppl.) to Number* **1:** 1–73.